EasyChair Preprint

№ 9485

Studying ZnS Nanoparticles as Buffer Layer for CdTe Solar Cells for Photovoltaic Application

Haytham El Farri, Amal El Yousfy and Mounir Fahoume

December 16, 2022

Studying ZnS nanoparticles as buffer Layer for CdTe solar Cells for photovoltaic application

Haytham EL FARRI,[a] **Amal EL YOUSFY, Mounir FAHOUME,**

[a] The Laboratory of Materials Physics & Subatomics, Department of Physics, Faculty of Sciences, Ibn Tofail University, BP 133 Kenitra, Morocco

(* corresponding author: haythamelfarri@gmail.com)

SUMMARY

Study of ZnS thin films prepared by Successive Ionic Layer Adsorption and Reaction (SILAR) Method

In this effort, we studied the possibility of replacing CdS buffer layer in CdTe solar cells thin films by ZnS nanoparticles. We start in first time to the literature and overview of ZnS materials and the common points with CdS thin films. Then we made simulations by SCAPS 1D Software to make sure if this material will respond as CdS buffer layer, speacelly in principal parameters: Thickness of the film and doping concentration with donors. Finally, Zinc Sulphide (ZnS) thin films were deposited on glass substrate by successive ionic layer adsorption and reaction (SILAR) method at room temperature (300 K). Zinc acetate and sodium Sulphide were used as cationic and anionic precursors for the films respectively. A study has been made for structural, surface morphological and optical properties of the film using X ray diffraction (XRD), EDX, scanning electron microscopy (SEM), and optical absorption method (UV). The deposited ZnS thin films showed polycrystalline with cubic phase. The SEM images of the films showed that films were uniformly distributed in substrates and homogeneous and the optical band gap was estimated of 3.52 eV.

KEY-WORDS: Buffer layer – SILAR - Thin films - Band gap - ZnS.

1. INTRODUCTION

The technology solar cell has seen enormous development during the last decades, originally for providing electrical power for spacecrafts and terrestrial applications [1]. The chief reason for this technology is the realization that the traditional fossil energy resources (coal, oil and gas) are rapidly depleting and contribute to possibly irreversible climate changes in the near future. The solar irradiation, has the advantage of being widely distributed over the world. Traditional silicon cell manufacturers are now constrained by the high prices, weight and fragility of silicon which presents the first generation of photovoltaic solar cells. Thin film solar cells, using inorganic or organic compounds as active layers, represent the promising technology for beating the cost of conventional silicon solar systems [2]. A thin film is a material created by the random nucleation and growth processes of individually condensing / reacting atomic / ionic / molecular species on a substrate. Thin-films encompass a considerable thickness range, varying from few nanometers to tens of micrometer [3]. Thin films solar cells, named also second generation of solar cells have many types forms like Copper Indium Gallium Di-Selenide CIGS, copper, indium and selenium CIS, Cadmium telluride CdTe (our case in this paper). The interest on the different properties of photonic CdTe material is of considerable, due to its importance in technological applications in x-ray imaging, solar energy conversion, optoelectronics, gamma ray detection, and integrated optics [4]. It can be doped with n-type or p-type and considering one of the leading materials thanks to its low cost and its high efficiency thin-film solar cells with a nearly ideal band gap of 1.48 eV for solar cell according to the Shockley-Queisser limit [5].

.

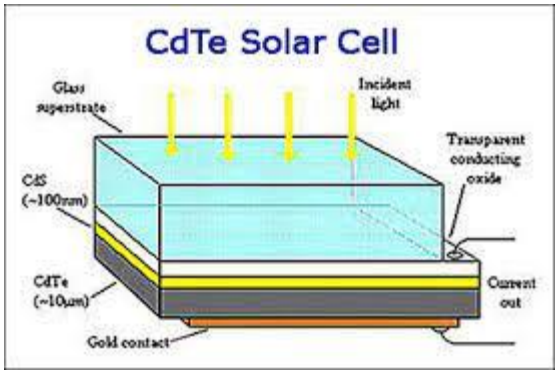

Figure 1. Transversal micrograph of CdTe solar cell [6]

The solar cells second generation are constitute of three principals layers: Absorber Layer (CdTe), Buffer Layer (ZnS) and Transparent Conducting Oxyde Layer (ZnO) . The background as we can see from the picture is Molybdenum (Mo), and up the TCO layer Glass substrate to protect the group of deterioration. At this stage, CdS is considered one of the most promising buffer layer for thin film heterojunction solar cells. Furthermore, the use of CdS thin films in large scale solar cell production could cause environmental problems due to high amount of waste from Cd compounds. Therefore, search for a Cd-free buffer layer materials have become a subject of interest and efforts geared towards overcoming these problems are still ongoing .The simulation of ZnS buffer layer in solar cells thin films has proved that this material is good candidate of CdS thin films [7]. Also thin films of ZnS have been successfully used as buffer layers to replace the CdS in CIGS based solar cells and have achieved a maximum efficiency of 19.71% [7] [8]. ZnS thin film is mostly suitable as a window layer in heterojunction photovoltaic solar cells; because the wide band gap reduces the window absorption losses and improves the short circuit current of

the solar cell. Researches have shown that ZnS is transparent to visible light, opaque to ultraviolet radiation and near infra-red radiations [9]. This material is an important semiconductor with a wide direct band gap and n-type conductivity is promising for optoelectronic device applications, such as electroluminescent devices and photovoltaic cells [10]. It is of interest for replacement of CdS as buffer layer in photovoltaic solar cells due to higher energy gap, good transparency, and general good film properties. From the literature, it is found that ZnS thin films have been deposited by physical methods like thermal evaporation, pulsed laser deposition, and chemical methods like Metal organic chemical vapor deposition, electrodeposition, sol gel, spray pyrolysis, chemical bath deposition [3]. In our case, we will use a simple technique named, SILAR (Successive Ionic Layer Adsorption and Reaction) technique-automatized, which is simple and economical because of the utilization of environment production conditions. It is considered as one of many methods in which thin films of compound semiconductors can be deposited by alternate dipping of a substrate into the aqueous solutions containing ions of each component [11]. The growth of ZnS thin films in the SILAR method occurs only heterogeneously on the solid–solution interface due to the intermediate rinsing step between the cation and anion immersions. This method is improved version of Chemical Bath Deposition (CBD). But in SILAR method, the precursor solutions are kept in different beakers. Hence it is easy to control the growth of the film. From the growth cycles, the controlled thickness can be possible. The deposition conditions were optimized for good quality and well adherent ZnS thin films. These films were characterized for their structural, morphological and optical properties by using X-ray diffraction, Scanning electron microscopy and optical absorption studies [12]. ZnS is with two main crystalline structures: one phase is the face-centered cubic lattice, also called a “zinc blende” type structure, when the second phase is a hexagonal structure, also called “wurtzite ZnS”, with the lattice belonging to the space group. In the first crystalline structure, each zinc atom is surrounded by four sulfur atoms, and each sulfur atom is surrounded by four zinc atoms in a tetrahedral coordination. In the second crystalline structure, wurtzite is characterized by 12 atoms in the corners of each unit that create a hexagonal unit cell, which is also tetrahedrally coordinated [13]. Since the zinc blende structure is denser than the wurtzite structure, a transition from zinc blende to wurtzite occurs naturally over time (extremely slow) at a rate similar to the transition of diamond to graphite. However, by thermal treatment, the cubic zinc blende can be transformed into a hexagonal structure (wurtzite) at 1020 ◦C. The purpose of this research is to study the structural and optical properties of ZnS thin films obtained by SILAR technique, deposited on glass substrate after annealing the samples at 350 C for 30 min.

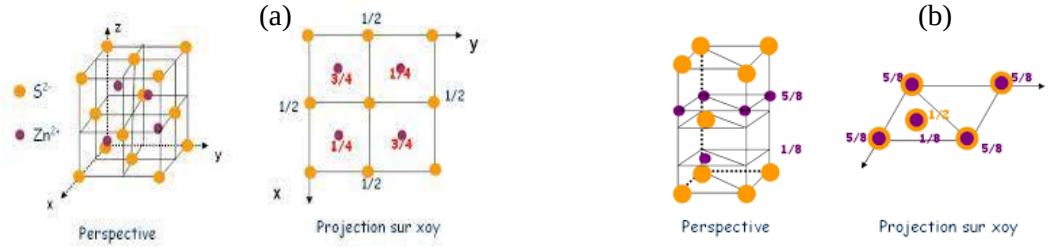

Figure 2. Crystallin structure of ZnS nanoparticles: (a) Blend Structure, (b) Wurtzite Structure.

2. NIMURICAL SIMULATION OF BUFFER LAYER BY SCAPS-1D SOFTWARE

The SCAPS software is a one dimensional solar cell simulation program developed at the department of Electronics and Information Systems (ELIS) of the University of Gent, Belgium. It is freely available and downloaded to the PV research community [14].

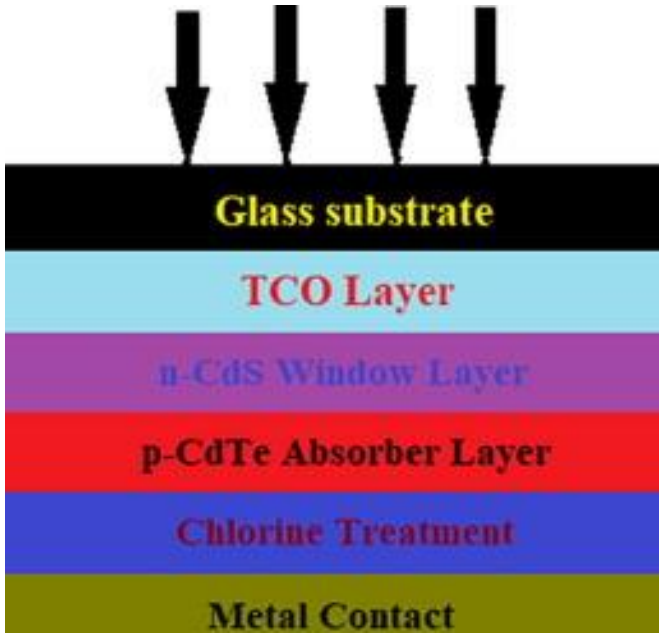

Figure 3. CdTe solar cells thin films [15]

Table 1. Input Parameter Values For The Simulation Of CdTe Solar Cells With SCAPS-1D.

Parameters	***i-ZnO***	***ZnS***	***CdTe***
Thickness (µm)	00.200	Varied	05.000
Band Gap (eV)	03.300	Varied	01.645
Electron Affinity (eV)	04.100	04.20	04.280
Dielectric Permittivity (relative)	09.000	10.000	09.400
CB Effective Density of States (cm^{-3})	4.000E+18	2.700E+18	8.000E+17
VB Effective Density of States (cm^{-3})	1.000E+19	1.800E+19	1.800E+19
Electron Thermal Velocity (cm/S)	1.000E+8	1.000E+7	1.000E+7
Hole Thermal Velocity (cm/S)	1.000E+8	1.000E+7	1.000E+7
Electron Mobility (cm^2/V.S)	1.000E+2	1.000E+2	3.200E+2
Hole Mobility (cm^2/V.S)	2.500E+1	2.500E+1	4.000E+1

The simulation is done under illumination the AM1.5, standard spectrum is used and the cell operating temperature is set at 300 K. We studied the effect of ZnS Buffer layer thickness and various doping effect on CdTe solar cells performance, in the hope to obtain optimal factors for making sophistical solar cells based with ZnS buffer layer.

2.1. Effect of ZnS buffer layer thickness on CdTe thin films

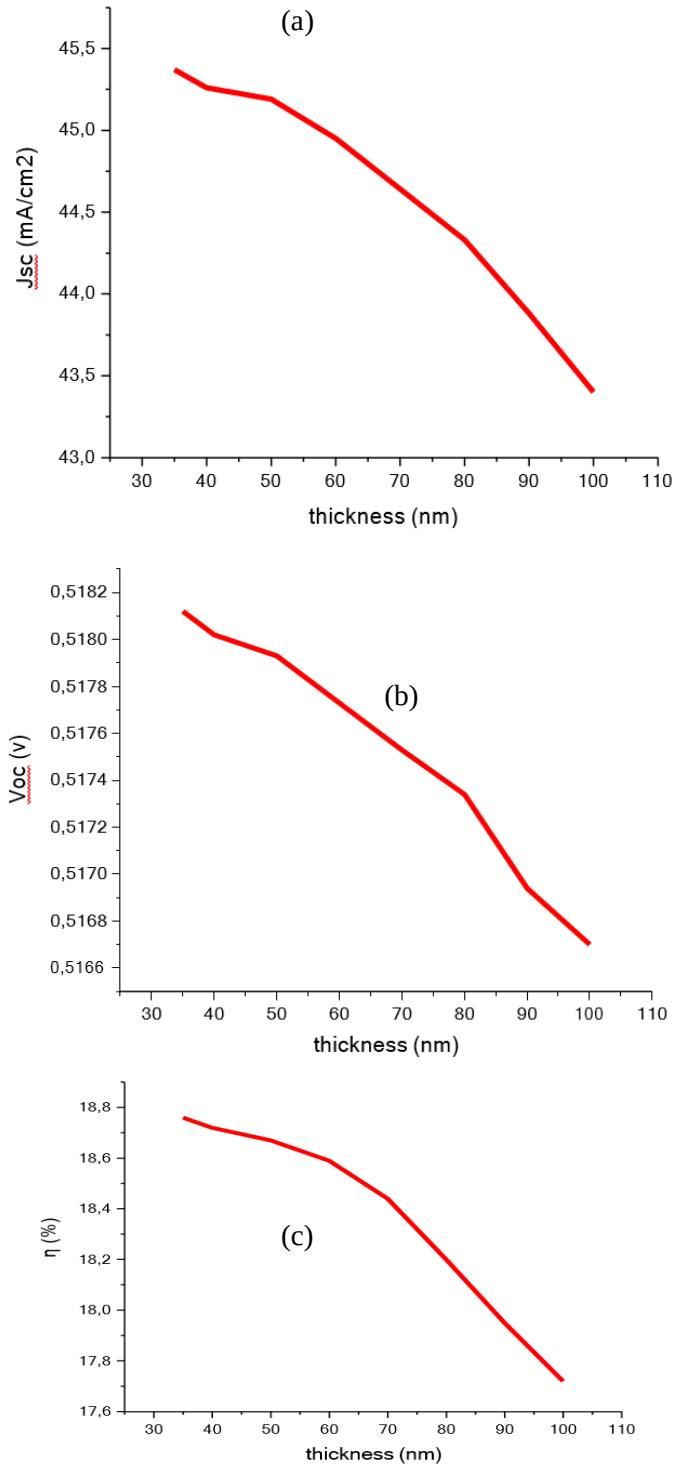

Figure 4. Effect of Thickness ZnS buffer layer on CdTe Thin films properties: (a) Short current density, (b) Open circuit voltage and (c) efficiency, by SCAPS 1D software.

We study in this part effect of Biffer layer thickness in CdTe solar cells, using SCAP 1D Software. The figure above shown the influence results of thickness layer on the functionning of solar cells

thin films. We have investigated the effects of this parameter on the CdTe performance solar cells: efficiency (η), open-circuit voltage (Voc) and short-circuit current density (Jsc). This is shown in Figure ‘’’, where the other layers properties are kept constant and the doping of ZnS layer is fixed at 10^{14} cm-3, while varying the ratio between ZnS layer thickness and absorber layer CdTe one’s (WZnS/WCdTe). When this factor increases, it affects severly the performance of CdTe thin films where we noted a drop of Voc, Jsc and η. When the rotio W_{ZnS}/W_{CdTe}, the Jsc varies from 45.328 mA/cm^3 for W_{ZnS}/W_{CdTe}= 0.6% to 43.311 mA/cm^3 for W_{ZnS}/W_{CdTe}= 2% with an important loss of 2.017 mA/cm^3. We can explain that loss by its corresponding to the loss in the absorption of the photons in the space charge region occurs in the ZnS layer due to the high band gap of this material (Eg=3.63eV), which is in agreement with other reports of ZnS Simulations [8] [16]

2.2. Effect of Various of ZnS Doping

The figure bellow shows various of short circuit current density (Jsc), open circuit voltage (Voc) and conversion efficiency (η) as a function of doping concentration ZnS nanoparticles with donors atoms. All parameters increase slightly with doping ZnS concentration. We can notice a decreasing of Jsc and Voc with concentration density of donors, when we can a critical point in η curve, with coordination of (E16 cm-3;18%). When the values of doping are under E16 cm-3, we constate an increasing of conversión efficiency, which is explaining mainly by the reduction of the width space charge region in the ZnS layer due to the augmentation of the Carrier concentration. Which increases the number photons absorbed in the absorber layer [17]. On the other hand, when doping concentration density is up than E16 cm-3, we notice a decreasing in the conversion efficiency, in this case, a significant amount of doping atom could not change the interstitial location in ZnS structure. As a result, the recombination rate has again increased, which reduced the efficiency of the device and in agreement with litterature of crystallographie of II-VI materials [18]

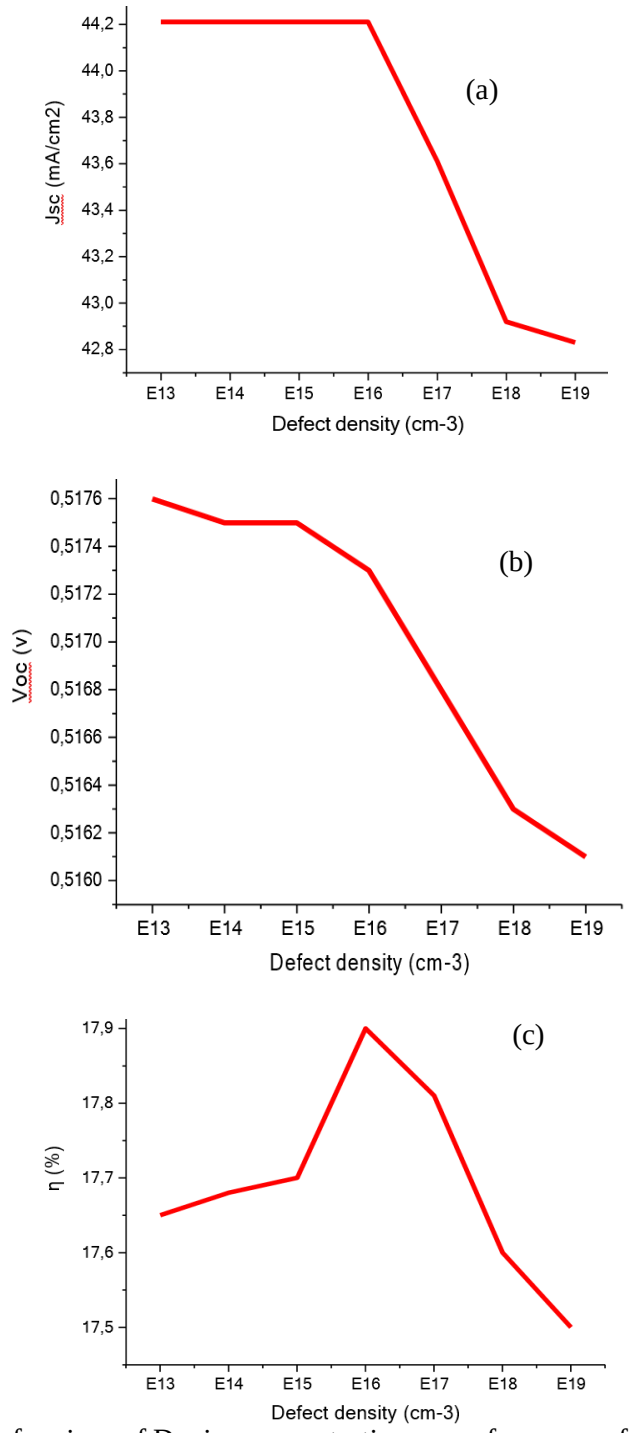

Figure 5. Effect of various of Doping concentration on performance of ZnS thin films by SCAPS 1D software: (a) Short current density, (b) Open circuit voltage and (c) efficiency, by SCAPS 1D software.

.

3. MATERIALS AND METHODS

3.1. Preparations of Substrates

The process of deposition was carried out by using Corning glass slides (25mm X 75mm X 1mm) as substrates. The substrates were ultrasonically cleaned with 20% hydrochloric acid, acetone and purified deionized water for 20 min, respectively. In the light of this deposition, cationic precursor used as zinc acetate ($Zn(CH_3COO)_2$) and anionic precursor as sodium sulphide (Na_2S). Well cleaned, glass substrates were dipped into aqueous solution of zinc acetate. The surface of the substrate was absorbed by zinc ions. Then substrate was rinsed by double distilled water to expulsion of loosely bound Zn^{2+} ions. Next step, the substrates were dipped into aqueous solution of sodium sulphide. The sulphide ions reacted with adsorbed zinc ions. Finally, to avoid precipitation the substrates were rinsed with distilled water. This is the growth cycle of SILAR method. To obtain desired thickness of the films, these growth cycles have been replicated.

The reactions involved were:

$$Zn(CH_3COO)_{2\ (Aqueous)} \rightarrow Zn^{2+}_{\ (Adsorbed)} + 2CH_3COO^-_{\ (In\ solution)}$$

$$Na_2S_{\ (Solid)} + H_2O \rightarrow 2Na^+ + SH^- \qquad (1)$$

$$OH^-_{\ (In\ solution)} + SH^-_{\ (In\ solution)} \rightarrow S^{2-}_{\ (In\ solution)} + H_2O$$

$$Zn^{2+}_{\ (In\ solution)} + S^{2-}_{\ (In\ solution)} \rightarrow ZnS_{\ (Adsorbed)} \qquad (2)$$

The prepared ZnS thin films were characterized to study structural and optical properties. Powder X-Ray diffraction analysis studied the crystal structure of the films. The surface feature of the films was analyzed by a scanning electron microscope (SEM). The UV - VIS spectrophotometer was used to measure the absorbance in the wavelength range 385 – 1100 nm and from these measurements, the band gap of the films was calculated. The exchange of cationic and anionic ions was modified by means of rinsing in double distilled water. In the SILAR technique, each cycle consists of i) adsorption of Zn^{2+} ions from Zinc acetate solution 30s, ii) rinsing with doubledistilled water for 20s, iii) reaction with sulphide precursor solution from thiourea solution for 30s and finally iv) rinsing with double distilled water for 20s. This operation was repeated for 50 times to get desired film thickness. The figure below shows the SILAR

controller coating with Stirrer in the laboratory of Materials physic and Subatomic in the department of physics of University Ibn Tofail-kenitra, Morocco.

Figure 6. The SILAR controller Coating with Stirrer.

After completion of film deposition, the sample was removed from the last beaker and immediately rinsed with de-ionized water to remove soluble impurities and evaporate the solvent and organic residues. After this step, the thin, uniform and colorless ZnS film is obtained. Than, the deposited film was annealed at 350^{o}C for 30 minutes to get good crystallinity of ZnS films.

2.2 Characterization of thin film

The structural characterization of the films was carried out using Philips Xpert-3 X-ray diffractometer with CuKα radiation (α= 1.540598 Å) in 2ɵ range from 050-900.The surface morphological study of ZnS films was carried out by scanning electron microscopy (SEM) using a model QUATTRO S-FEG-Thermofisher scientific operating at a voltage of 20 KV uses the BSE detector and Energy dispersive X-ray analysis (EDS) were recorded on Energy dispersive X-ray spectrometer attached to the SEM model. The preparative parameters for best quality ZnS thin films were optimized as illustrated in Table 1.

Table 2. Optimized preparative parameters for ZnS thin films deposited on glass substrate.

Parameters	Precursors solutions	
	Zinc acetate	**Sodium Sulphid**
Concentration (M)	0.15	0.15
PH	~ 10	~ 10
Immersion time (S)	30	30
Rinsing time (S)	20	20
Number of SILAR cycle	50	50
Temperature (K)	298	298

4. RESULTS AND DISCUSSION

4.1. Structural Studies

To study the crystal structure of ZnS film deposited by SILAR method, we examine X-ray diffractogram of the film onto glass substrate. Zinc Sulphide can be grown with either hexagonal, wurtzite type structure or the cubic zinc blende-type structure. After the annealing temperature up to 350° C for 30 minutes, the previous report on chemically deposited ZnS film showed that this film is polycrystalline. The XRD patterns of the sample is shown in Figure 2. The pattern shows polycrystalline structure with cubic phase and peaks correspond to (111), (220) and (311) planes. The XRD pattern of as-deposited film with poor crystallinity, since no well-resolved peaks were observed at $2\theta = 29.18°$ (111), $2\theta = 48.33°$ (220) and $2\theta = 57.64°$ (311) over a wide base that corresponds to Blend structure phase of ZnS. The high intensity and diffraction peak shows that the as-deposited ZnS thin film is polycrystalline thanks to the annealing temperature of our ZnS sample. The XRD peaks are broadened due to nanocrystalline nature of ZnS sample [19].

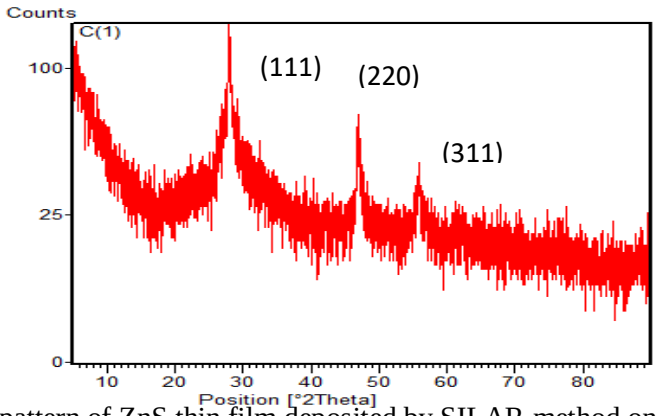

Figure 7. XRD pattern of ZnS thin film deposited by SILAR method onto glass substrate for 50 cycles at room Temperature.

The observed XRD pattern is in agreement with standard data JCPDS. The XRD data were used to determine the crystallite size (D), dislocation density (δ) and micro strain (ε) of the (111) diffraction plane. The crystallite size was calculated using Debye-Scherer formula [20]:

$$D=\frac{k\lambda}{\beta\cos\theta} \qquad (1)$$

Where:

k is approximately equal to 0.94, λ is the wavelength of X ray (1.5406 Å), β is the width of the most intense peak at half maximum intensity and θ is the diffraction angle.

The dislocation parameter is a crystallographic defect, presents an irregularity within a crystal structure. The presence of dislocations (δ) strongly influences many of the properties of materials. We can define the dislocation density of our ZnS sample by the formula below [21]:

$$\delta=\frac{1}{D^2} \qquad (2)$$

Where the D is the crystallite size of our material.

The micro strain ε in the film was determined using the relation [1]:

$$\varepsilon=\frac{\beta\cos\theta}{4} \qquad (3)$$

The calculated value of the crystallite size, dislocation density, and micro strain 70.74 nm; 1.993×10^{14} line/m^2 and 4.09×10^{-3}.

4.2. Surface Morphological Studies

The scanning electron microscopy technique is specific method for the study of surface morphology of thin film form. The ZnS film prepared with optimized parameters is used for

Scanning Electron Microscopy (SEM) observation. Figure 3 shows the SEM micrograph of ZnS thin film. We can notice that the film is homogeneous, well adherent and covers glass substrate without cracks. The film compactness is high, the grain size is generally small and they are agglomerated in some places. Also, the surface morphology of the deposited ZnS films were uniformly distributed on the surface of substrate with enlarged irregular shape with smaller pin holes, while it shows uniform, compact, homogenous, and composed of nearly spherical shaped grains distribute on the surface of substrate [22]. From the table of material composition of ZnS thin films, we can notice that the ratio weight was estimated of 0.44 of the weight percent for Zn and S respectively as shown in Table 2. The EDS spectrum also shows that the prepared films are relatively free from impurities. The presences of O element is probably due to glass substrate (SiO_2), when the presence of Carbone element is due to Zinc Acetate precursor no completely reacted.

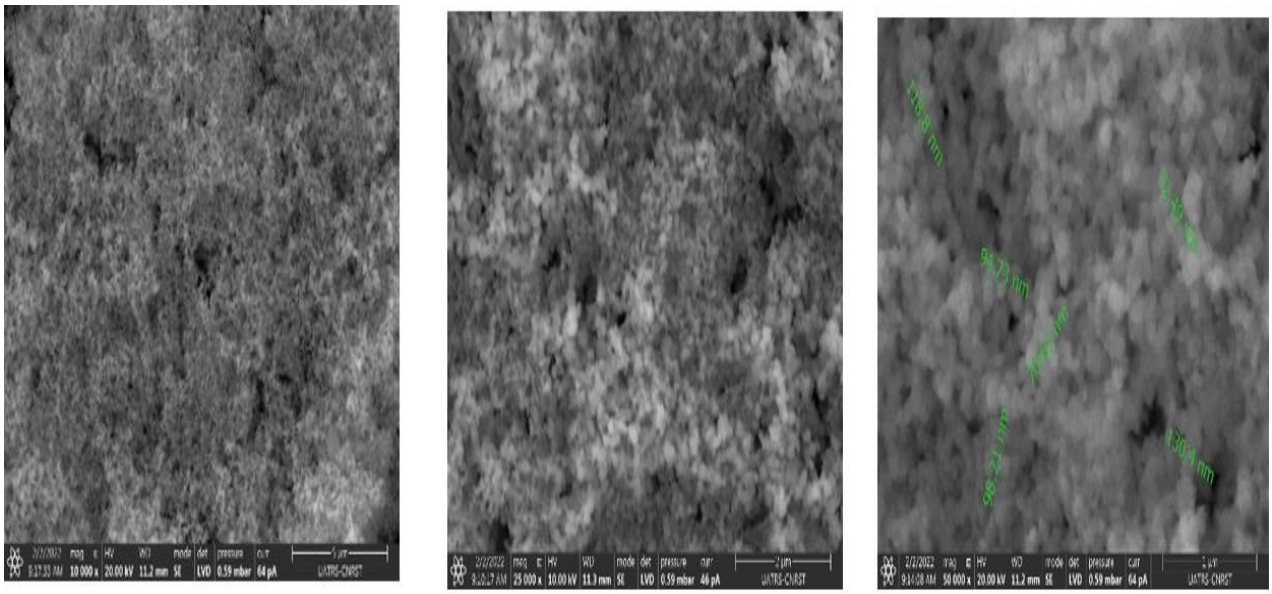

Figure 8. SEM image of as-deposited ZnS film on glasssubstrate at room temperature.

The EDS technique is used to determine quantitative composition of ZnS films deposited on glasssubstrate [23]. The presence of EDS peaks for Zn and S are conformed from analysis (figure 4).

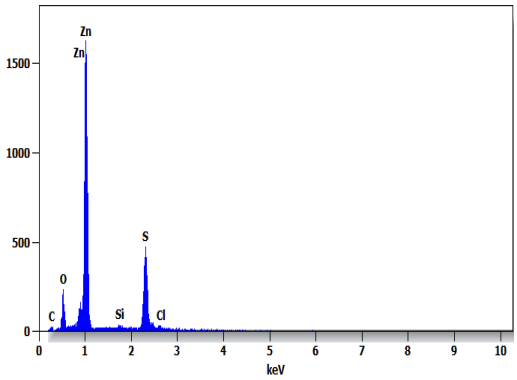

Figure 9. The EDS analysis of as- deposited ZnS on glass substrate at room temperature.

Table 3.Elemental analysis of as-deposited ZnS thin film.

Element	*Weight %*	*Atom % Error*
C	0.69	± 0.55
O	1.78	± 0.44
S	29.65	± 0.58
Zn	67.88	± 0.50
Total	100.00	

3.3 The Optical Properties

The optical transmission spectra of ZnS film deposited on glass substrate at room temperature is shown in fig.5. The spectra reveals that the transmittance is high in the visible/near infrared region from 338-900 nm. The high transmittance of the films is a consequence of the wide band gap. We can notice that the higher transmittance indicates a fairly smooth surface and relatively good homogeneity of the film. Also, the high transmittance of the films in the visible range is very important for optical applications. The spectra of transmission obtained in our sample is composed of two different regions: a region of strong absorption ($\lambda <$ 380 nm), corresponding to fundamental absorption in thin film of ZnS, which is due to the electronic transition inter band. The variation of the transmission in this region is exploited for the determination of the optical band gap energy and the disorder. In the second region of strong transparency ($\lambda >$ 380 nm): the value of the transmission is about 25% to 45% in the wavelength range of 380–850 nm. We noticed that transmittance spectra of our ZnS sample has no interference fringe due to the incident light scattering in the material because of interface air/film roughness [24] .

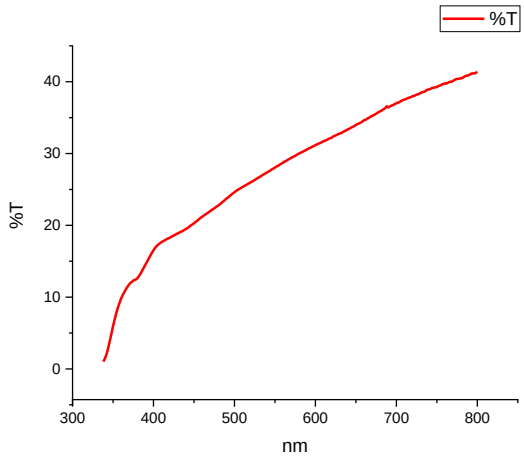

Figure 10. The transmittance spectra of as-deposited ZnS thin film on glass substrate.

The absorption measurement was carried out after the sulfurization and annealing the sample at high temperature of 350 C for 30 min. To determine the energy band gap, we plotted $(\alpha h\nu)^2$ vs.$(h\nu)$, where α is the absorption coefficient and $h\nu$ is the photon energy. The theory of inter band absorption shows that at the optical absorption, edge the absorption coefficient α varies with the photon energy $h\nu$ according to the Ref [25].

$$\alpha\ (h\nu)=A(h\nu-E_g)^{1/2}$$

where: A is a constant and Eg is the optical band gap. This graph $(\alpha h\nu)^2$ vs hν has been given in figure 6. The band gap energy of ZnS thin film has been determined by the extrapolation of the linear regions on the energy axis (hν). We can constate after the application of Tauc Law on the first region of ZnS transmittance, that the band gap energy value (Eg=3.52 eV) is lower than that of bulk value of ZnS (3.7 eV). The wide band gap energy which is the reason of window layer absorption decreases loses and consequently these yields to the solar cell short circuit current improvement.

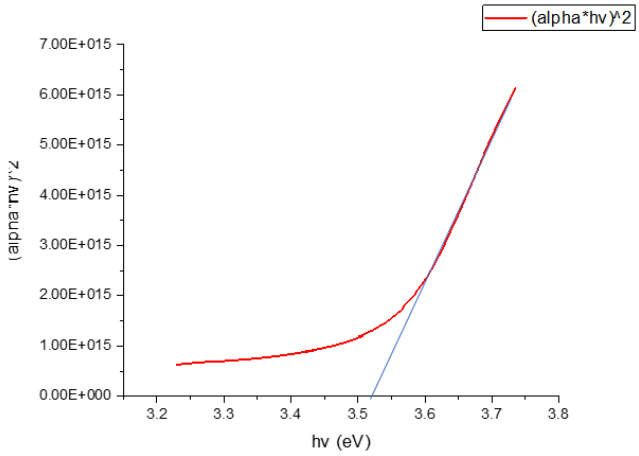

Figure 11. Absorbance spectra of as-deposited ZnS thin film on glass substrate at room temperature.

The refractive index (n) of ZnS thin films elaborated on glass substrate is calculated using the model of Herve-Vandamme [26]:

$$n^2=1+\left(\frac{A}{B+E_g}\right)^2$$

Where A and B are constants: A ≈ 13.6 eV and B ≈ 3.4 eV.
Eg is the experimental values of gap optic energy.
We found that value of the refractive index (n) is 2.2045.

5. CONCLUSIONS

In this paper, we studied the theory of Buffer layer candidate (ZnS)to replace the standard buffer layer used in CdTe Solar cells application.

Thanks to SCAPS, we confirmed that ZnS presents good alternative material o f CdS Buffer layer, which is constituting a danger and cancer material for environment and for people

We discussed also experimental part of ZnS nanocrystalline films were grown on glass substrates using SILAR Technique automatized. The band gap of nanocrystalline ZnS was found 3.52 eV, which is in agreement with the literature.

The results of structural, morphological and optical properties, have been successfully discussed. Also, the morphology of the surface shows that the films are uniform throughout the surface and The EDX analyses revealed that Zinc (Zn) and Sulphur (S) are present in the films with 67.88% and 29.65% by weight, respectively.

We can notice in our case that the deposited ZnS thin film can be good candidate for optoelectronic devices especially in Buffer layer of photovoltaic cells.

ACKNOWLEDGMENTS

I would like to express my gratitude to the member of Laboratory of Materials Physics & Subatomic, from department of physics of University Ibn Tofail, for their collaboration and their guidance to treat this paper with high quality.

I would like to express my deep gratitude to Professor Mounir FAHOUME and Professor Khalid NOUNEH, my research supervisors, for their patient guidance, enthusiastic encouragement and useful critiques of this research work.

References

[1] E. A.-E. Mohammad Ali Mohtadi-Bonab *et al.*, "Synthesis and Characterization of aluminum dope zinc sulfide (Al:ZnS) thin films by chemical bath deposition techniques.," *Chalcogenide Lett.*, pp. 1–6, 2021.

[2] O. Osanyinlusi, "Preparation and Characterization of ZnS Thin Films Grown by Spin Coating Technique.," *Tanzania J. Sci.*, pp. 534–547, 2020.

[3] T. V. T. Shobana, "A Comprehensive Review on Zinc Sulphide Thin Film by Chemical Bath depositions techniques," *J. Environ. Nanotechnol.*, pp. 50–59, 2020.

[4] S. C. Ray and K. Mallick, "Cadmium Telluride (CdTe) Thin Film for Photovoltaic Applications," *Int. J. Chem. Eng. Appl.*, vol. 4, no. 4, pp. 183–186, 2013, doi: 10.7763/ijcea.2013.v4.290.

[5] "Enhancing CdTe Solar Cell Performance by Reducing the 'Ideal' Bandgap of CdTe through CdTe".

[6] S. Chander and M. S. Dhaka, "Preparation and physical characterization of CdTe thin films deposited by vacuum evaporation for photovoltaic applications," *Adv. Mater. Lett.*, vol. 6, no. 10, pp. 907–912, 2015, doi: 10.5185/amlett.2015.5926.

[7] M. B. (2021). H. Elfarri, "Optimization of simulations of thickness layers, temperature and defect density of CIS based solar cells, with SCAPS-1D software, for photovoltaic application.," *Chalcogenide Lett.*, pp. 201–213, 2021.

[8] M. B. (2021). H. El Farri, "Theoretical simulation of ZnS buffer layer thin films with SCAPS-1D software for photovoltaic applications," *Chalcogenide Lett.*, pp. 457–465, 2021.

[9] S. D. Tizazu Abza, "Characterization of CdS/ZnS and CdS/CoS Multilayer Thin Films Synthesized by Chemical Bath Deposition.," *Int. J. Thin Film Sci. Technol. J.*, pp. 1–6, 2021.

[10] T. A. (2021) Gemechis Megersa Jigi, "Synthesis and Characterization of

aluminum dope zinc sulfide (Al:ZnS) thin films by chemical bath deposition techniques," *J. Appl. Biotechnol. Bioeng.*, pp. 55–58, 2021.
[11] M. A. Jesu Jebathew, "High sensitive samarium-doped ZnS thin films for photo-detector applications," *Opt. Mater. (Amst).*, pp. 1–9, 2021.
[12] I. H. Nisreen S. Turki, "Optical properties of ZnS and PEDOT thin films.," . *AIP Conf. Proceedings.*, 2021.
[13] A. P.-H.-R. I. J. González-Chan, "Synthesis and characterisation of ZnS thin films obtained without complexing agent by the chemical bath technique.," *Surf. Engeenering*, pp. 1120–1132, 2021.
[14] M. Burgelman, K. Decock, A. Niemegeers, J. Verschraegen, and S. Degrave, "SCAPS Manual," *Univ. Gent*, no. february, pp. 1–111, 2019.
[15] S. Chander and M. S. Dhaka, "Enhancement in microstructural and optoelectrical properties of thermally evaporated CdTe films for solar cells," *Results Phys.*, vol. 8, pp. 1131–1135, 2018, doi: 10.1016/j.rinp.2018.01.055.
[16] H. Elfarri, M. Bouachri, A. Frimane, M. Fahoume, O. Daoudi, and M. Battas, "Optimization of simulations of thickness layers, temperature and defect density of cis based solar cells, with scaps-1d software, for photovoltaic application," *Chalcogenide Lett.*, vol. 18, no. 4, pp. 201–213, 2021.
[17] N. Touafek, R. Mahamdi, and C. Dridi, "Impact of the secondary phase ZnS on CZTS performance solar cells," vol. 9, pp. 6–9, 2019.
[18] Shahar Bano *et al.*, "Effect of Cd doping on the structural, optical, and photovoltaic properties of SnS films," *J. Mater. Res. Technol.*, vol. 19, pp. 1982–1992, 2022, doi: 10.1016/j.jmrt.2022.05.137.
[19] D. R. DivyaAgrawal, "Achieving desired quality of ZnS buffer layer by optimization using air annealing for solar cell applications.," *Phys. Lett. A.*, 2020.
[20] A. S. A O Bokuniaeva, "Estimation of particle size using the Debye equation and the Scherrer formula for polyphasic TiO2 powder.," . *J. Phys. Conf. Ser. , 1-6.*, pp. 1–6, 2019.
[21] Y. S. (2009). N.A. Koneva, "Parameters of Dislocation Structure and Work Hardening of Ni 3 Ge.," *Mater. Res. Soc.*, pp. 1–6, 2009.
[22] A. A.-A.-S. AhmedAL-Osta, "Structural, morphological and optical properties of Cr doped ZnS nanoparticles prepared without any capping agent," *Optik (Stuttg).*, 2020.
[23] E. Y. Stanislav I. Sadovnikov, "Synthesis and Characterization of (Ag2S)x(ZnS) Heteronanostructures.," *IOP Conf. Ser. Mater. Sci. Eng.*, pp. 1–5, 2019.
[24] R. R. Rahul Singh, "Optical Properties of ZnS Quantum Dots: Applications in Solar cells and Biomedicine.," *Biointerface Res. Appl. Chem.*, pp. 1–9, 2022.
[25] J. Z. Dejan Zagorac, "Band Gap Engineering of Newly Discovered ZnO/ZnS Polytypic Nanomaterials.," *nanomaterials*, pp. 1–20, 2022.
[26] A. M. SubhashChander, "Enhancement of optical and structural properties of vacuum evaporated CdTe thin films.," *Mater. Chem. Phys.*, pp. 202–209, 2017.